



Tricritical point in the mixed-spin Blume-Capel model on three-dimensional lattices: Metropolis and Wang-Landau sampling approaches

Mouhcine Azhari ^{*}

*Fakultät für Mathematik und Naturwissenschaften Bergische Universität Wuppertal, 42097 Wuppertal, Germany
and Laboratory of High Energy Physics and Condensed Matter, Hassan II University-Casablanca, Faculty of Sciences Ain-Chock, 5366
Maarif, Casablanca 20100, Morocco*

Unjong Yu [†]

Department of Physics and Photon Science, Gwangju Institute of Science and Technology, Gwangju 61005, South Korea

 (Received 9 December 2019; revised 15 June 2020; accepted 9 September 2020; published 12 October 2020)

We investigate the mixed-spin Blume-Capel model with spin-1/2 and spin- S ($S = 1, 2$, and 3) on the simple cubic and body-centered cubic lattices with single-ion-splitting crystal field (Δ) by using the Metropolis and the Wang-Landau Monte Carlo methods. We show that the two methods are complementary: The Wang-Landau algorithm is efficient to construct phase diagrams and the Metropolis algorithm allows access to large-sized lattices. By numerical simulations, we prove that the tricritical point is independent of S for both lattices. The positions of the tricritical point in the phase diagram are determined as $[\Delta_t/J = 2.978(1); k_B T_t/J = 0.439(1)]$ and $[\Delta_t/J = 3.949(1); k_B T_t/J = 0.854(1)]$ for the simple cubic and the body-centered cubic lattices, respectively. A very strong supercritical slowing down and hysteresis were observed in the Metropolis update close to first-order transitions for $\Delta > \Delta_t$ in the body-centered cubic lattice. In addition, for both lattices we found a line of compensation points, where the two sublattice magnetizations have the same magnitude. We show that the compensation lines are also S independent.

DOI: [10.1103/PhysRevE.102.042113](https://doi.org/10.1103/PhysRevE.102.042113)

I. INTRODUCTION

The Ising model [1] can be solved analytically on one- and two-dimensional lattices [2]. Despite tremendous efforts in the past few decades, there is unfortunately no analytic solution in three dimensions (for a recent review, see Ref. [3]). It exhibits a simple critical point and its properties are now well known. Other models that have multicritical points are generally less well understood. Interesting features may arise when one considers more than two states, and the Blume-Capel (BC) model [4,5] is one of the simplest extensions that realizes a tricritical Ising point where three different phases become indistinguishable. This Ising model with allowed vacant sites has attracted particular attention in connection with its wetting and interfacial adsorption under the presence or absence of bond randomness [6–9]. It consists of a spin-1 Ising Hamiltonian with an anisotropy field Δ (also called single-ion-splitting crystal field). The latter term controls the density of vacancies and plays a dominant role in the existence of the tricriticality. It allows the model to have a nontrivial tricritical point (TCP) in two- and three-dimensional lattices [10–17]. However, couplings must be fine-tuned and then simulations have extreme difficulty in finding the precise location of such a point in a multidimensional space of coupling constants due to the exceptionally large fluctuations in the order parameter

close to the TCP [10,18]. On the other hand, in the case of the BC model, the presence of an almost vertical slope in the vicinity of the TCP allows to cross the phase diagram at fixed temperatures along the crystal-field axis. For the three-dimensional ferromagnetic BC model, the coordinates of the TCP can be located with fairly high accuracy using a microcanonical Monte Carlo technique [11], whereas precise data of the thermodynamic properties in both the first- and second-order phase boundaries can be obtained by parallelization of multicanonical simulations [14,19,20].

It should also be stressed that two is the lower tricritical dimensionality of BC systems. However, this situation changes radically when we consider a mixture of spin 1/2 and spin S , since they have less translational symmetry than their single-spin counterparts. This latter property has a great influence on the magnetic properties of the mixed-spin systems and causes them to exhibit unusual behavior not observed in single-spin Ising models [21]. These mixed-spin models have already found various applications for the description of certain types of ferrimagnetism, such as the $\text{MnNi}(\text{EDTA})\cdot 6\text{H}_2\text{O}$ complex and the two-dimensional compounds $A^I M^{II} \text{Fe}^{III} (\text{C}_2\text{O}_4)_3$ [$A = \text{N}(n\text{-C}_3\text{H}_7)_4, \text{N}(n\text{-C}_4\text{H}_9)_4, \text{N}(n\text{-C}_5\text{H}_{11})_4, \text{P}(n\text{-C}_4\text{H}_9)_4, \text{P}(\text{C}_6\text{H}_5)_4, \text{N}(n\text{-C}_4\text{H}_9)_3(\text{C}_6\text{H}_5\text{CH}_2), (\text{C}_6\text{H}_5)_3\text{PNP}(\text{C}_6\text{H}_5)_3, \text{As}(\text{C}_6\text{H}_5)_4; M^{II} = \text{Mn, Fe}$] [22,23].

In recent years, much controversy has surrounded the behavior of the mixed-spin BC model in two dimensions [24–33]. Up to now, it has been explored in two varieties of analytical approaches [33–35]. The first one is to use an

^{*}azhari.mouhcine@gmail.com

[†]Corresponding author; uyu@gist.ac.kr

exact mapping transformation, which maps the subject model on the honeycomb and Lieb lattices onto an exactly solved one with effective mapped interaction [34,35]. The second one was proposed recently based on a heuristic approach to solve the same model on the square lattice [33]. As a result, it turned out that in two-dimensional bipartite lattices the mixed-spin BC model has neither tricritical nor compensation points, as had been suggested by previous approximative approaches [24,25,27,29,31]. These findings are in full agreement with the Monte Carlo (MC) simulations [28,30,32,36] and the renormalization-group method [26].

In contrast, there is no exact result in three-dimensional cases. Selke and Oitmaa [32] have performed MC simulations for the Blume-Capel model with mixed spin-1/2 and spin-1 on the simple cubic (SC) lattice applying the Metropolis update (MU) of single-spin flips [37] and long runs. They found evidence for a tricritical point (TCP) and a line of compensation points. This is consistent with the renormalization-group calculations [38], which indicates the existence of the TCP in the phase diagram. In Ref. [32], the location of the TCP was obtained tentatively based on the histogram of the magnetization in a small system. We show in this paper that such a small lattice size leads to an underestimation in locating the TCP, which calls for a more extensive study on this model.

Our purpose here is to study two lattices to better improve our understanding of the mixed-spin systems. Motivated by this, we re-examine the mixed-spin Blume-Capel model on the SC lattice using the standard MU [37] and the Wang-Landau (WL) algorithm [12,13,15,39]. As far as we know, the WL algorithm has never been implemented to study mixed-spin systems. We show that the two methods are complementary to each other. We propose a reliable method to locate the TCP for the mixed spin-1/2 and spin-1 Blume-Capel model on the SC lattice. The cases of $S = 2$ and 3 are also studied, and the S dependence of the TCP is discussed. The same method is applied to the body-centered cubic (BCC) lattice to locate the TCP for integer S . In addition, we show that both lattices exhibit compensation phenomena, which can be very useful in magnetic memory and spin analyzing applications [40].

The outline of the article is as follows. As necessary background, in Sec. II we introduce the mixed-spin Blume-Capel model and summarize the numerical details of our simulations. In Sec. III, we discuss our results for both lattices SC and BCC, and we present our analysis for the cases $S = 1, 2$, and 3 . We then conclude with a summary in Sec. IV.

II. MODEL AND METHODS

We studied the mixed-spin Blume-Capel model on the SC and BCC lattices. The Hamiltonian can be written as

$$H = -J \sum_{(i \in \Lambda_1, j \in \Lambda_2)} \sigma_i S_j + \Delta \sum_{j \in \Lambda_2} (S_j)^2. \quad (1)$$

Each lattice consists of two interpenetrating sublattices Λ_1 with the spin variables σ_i and Λ_2 with spins S_j . Spins σ_i and S_j may take on the values $\pm 1/2$ and $\{-S, -S + 1, \dots, S\}$, respectively, where S is an integer or half-integer greater than $1/2$. In this paper, we study only integer S cases ($S = 1, 2$, and 3). The notation $\langle i \in \Lambda_1, j \in \Lambda_2 \rangle$ stands for summation

over all pairs of nearest-neighbor spins. The exchange interaction J is between two nearest neighbors σ_i and S_j , and Δ is the single-spin anisotropy. Positive J means that the interaction is ferromagnetic. Since the lattices we study in this paper are bipartite, ferrimagnetic case ($J < 0$) is completely equivalent to the ferromagnetic case. In this work, all the results presented in this paper are obtained for $J > 0$.

We consider three-dimensional cubic lattices SC and BCC with the number of lattice points $N = BL^3$, where L is the linear size of the system and B is the number of sites per unit cell. For the SC and BCC lattices, $B = 1$ and $B = 2$, respectively. With this definition in mind, what we called the SC (respectively, BCC) lattice is in fact the face-centered-cubic (respectively, SC) Bravais lattice. The periodic boundary condition is used in all directions. We used two kinds of MC schemes: the MU [37] and WL sampling [12,13,15]. The MU is simple, easy to implement, and provides access to simulations in large lattice sizes, but it suffers from critical and supercritical slowing down [41] and it is not reliable close to first-order transitions. In contrast, the WL sampling overcomes the critical and supercritical slowing down and eliminates hysteresis. Besides, physical quantities for any temperature and anisotropy can be obtained just by one calculation, but the lattice size is limited in the WL method due to the multiparametric Hamiltonian of our model and hence the huge number of the energy levels, which increases with S . The maximum lattice size studied in this work is $L = 100$ and $L = 10$ for the MU and WL methods, respectively. The MU has been widely used in both single- and mixed-spin systems [42] and we shall only discuss the relatively new method, the WL sampling.

The WL sampling method directly estimates the density of states $\rho(E_1, E_2)$ via a random walk in energy space with the transition probability

$$P[(i_1, i_2) \rightarrow (j_1, j_2)] = \min \left[1, \frac{\rho(E_{i_1}, E_{i_2})}{\rho(E_{j_1}, E_{j_2})} \right], \quad (2)$$

which makes histogram $h(E_1, E_2)$ flat. The two energy variables E_1 and E_2 represent the two terms of the Hamiltonian in Eq. (1), respectively:

$$E_1 = \sum_{(i \in \Lambda_1, j \in \Lambda_2)} \sigma_i S_j \text{ and } E_2 = \sum_{j \in \Lambda_2} (S_j)^2. \quad (3)$$

The splitting choice is specific to the BC model, as it was first introduced by Silva *et al.* [12] and then generalized to other models with multienergy variables [43,44]. The purpose of this choice is to overcome the barriers in both energy spaces. Therefore, the energy space ξ of the density of states $\rho(E_1, E_2)$ is proportional to the size of the system L and the spin variables S as $\xi = (zSN/2)(S^2N/2) = (zB^2/4)L^6S^3$, where z is the coordination number, about half of ξ has nonzero density of states. We found that the CPU time required to get the density of states is roughly proportional to ξ^α with $\alpha = 1.26(4)$; it takes about eight hours for $L = 10$ and $S = 1$ in the SC lattice on a 2.2-GHz Intel(R) Xeon(R) processor.

At each step, the WL refinement is $\rho(E_1, E_2) \rightarrow f_n \rho(E_1, E_2)$, where $f_n > 1$ is an empirical factor. Whenever the energy histogram is flat enough, the modification factor

f_n is adjusted as $f_{n+1} = \sqrt{f_n}$ with $f_0 = e$ and a new set of random walks is performed. The whole simulation is terminated when f_n becomes close enough to 1: $f_{\text{final}} < \exp(10^{-10})$. See Ref. [45] for more detail. During the simulation, average values of thermodynamic observables $O(E_1, E_2)$ as a function of E_1 and E_2 should be calculated.

Once the density of states $\rho(E_{i_1}, E_{i_2})$ is obtained, the partition function can be calculated for any values of temperature and anisotropy,

$$Z(T, \Delta) = \sum_{E_1, E_2} \rho(E_1, E_2) e^{\beta(JE_1 - \Delta E_2)}, \quad (4)$$

where β denotes the inverse temperature $1/k_B T$ and k_B is the Boltzmann constant. It is straightforward that all thermodynamic observables $\langle O \rangle(T, \Delta)$ can be calculated without additional simulation for each temperature and anisotropy:

$$\langle O \rangle(T, \Delta) = \frac{1}{Z} \sum_{E_1, E_2} O(E_1, E_2) \rho(E_1, E_2) e^{-\beta H}. \quad (5)$$

To map the phase diagram, we calculated the sublattice and the total magnetizations

$$\langle M_\sigma \rangle(T, \Delta) = \frac{1}{Z} \sum_{E_1, E_2} M_\sigma(E_1, E_2) \rho(E_1, E_2) e^{-\beta H}, \quad (6)$$

$$\langle M_S \rangle(T, \Delta) = \frac{1}{Z} \sum_{E_1, E_2} M_S(E_1, E_2) \rho(E_1, E_2) e^{-\beta H}, \quad (7)$$

$$\langle M \rangle(T, \Delta) = \frac{1}{Z} \sum_{E_1, E_2} M(E_1, E_2) \rho(E_1, E_2) e^{-\beta H}, \quad (8)$$

where $M_\sigma(E_1, E_2)$, $M_S(E_1, E_2)$, and $M(E_1, E_2)$ are averages of the microcanonical sublattice and total magnetizations for given E_1 and E_2 :

$$\begin{aligned} M_\sigma(E_1, E_2) &= \frac{\sum_{v=1}^{V_{E_1 E_2}} |\sum_{i \in \Lambda_1} \sigma_i(v)|}{V_{E_1 E_2} N_\sigma}, \\ M_S(E_1, E_2) &= \frac{\sum_{v=1}^{V_{E_1 E_2}} |\sum_{j \in \Lambda_2} S_j(v)|}{V_{E_1 E_2} N_S}, \\ M(E_1, E_2) &= \frac{\sum_{v=1}^{V_{E_1 E_2}} |\sum_{i \in \Lambda_1} \sigma_i(v) + \sum_{j \in \Lambda_2} S_j(v)|}{V_{E_1 E_2} N}, \end{aligned} \quad (9)$$

where $V_{E_1 E_2}$ is the number of visits to states of (E_1, E_2) during the process of the WL sampling; $\sigma_i(v)$ and $S_j(v)$ are the spin values of sites i and j , respectively, for the v th visit [12,15]. Since the random walk is performed to estimate the density of states $\rho(E_1, E_2)$ in the WL algorithm, we do not need extra random walks for the calculation of the magnetization. (In order to reduce the statistical error, extra random walks can be performed after $\rho(E_1, E_2)$ is determined [15], but we found that such extra processes have a little effect on the final results.) Therefore, the additional computational burden to calculate $\langle M_\sigma \rangle$, $\langle M_S \rangle$, and $\langle M \rangle$ is minor. Note that $N_\sigma = N_S = N/2$ for the SC and BCC lattices. In addition, to locate the critical temperature T_C and to determine the type of transition, we calculated the Binder cumulant [46]

$$U = 1 - \frac{\langle M^4 \rangle}{3 \langle M^2 \rangle^2}. \quad (10)$$

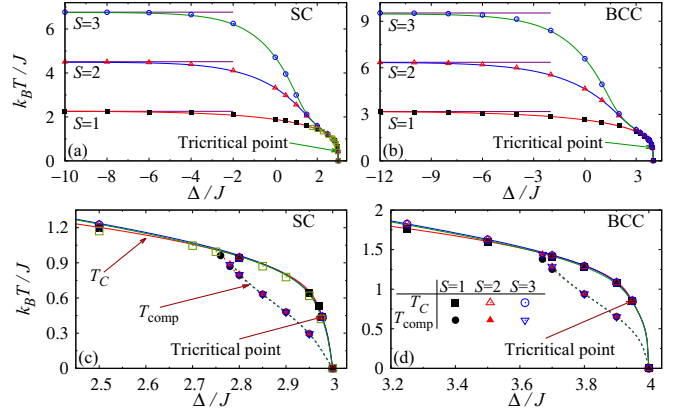


FIG. 1. Phase diagram in the Δ - T plane for the SC ((a) and (c)) and BCC ((b) and (d)) lattices. Compensation temperature (T_{comp}) is represented with dashed lines in lower panels. The horizontal straight lines represent $T = (S/2)T_C^{\text{Ising}}$, which is the critical temperature expected in the limit $\Delta \rightarrow -\infty$. T_C^{Ising} is the critical temperature of the conventional Ising model in the SC and BCC lattices. The transition temperature (T_C) and the compensation temperature (T_{comp}) were obtained by using the WL (solid and dashed lines) and MU (symbols). The statistical error is smaller than the symbol size. Previous results of the transition temperature by Selke and Oitmaa [32] in the SC lattice are also shown by the empty squares.

III. RESULTS AND DISCUSSION

Figure 1 shows phase diagrams in the T - Δ plane for the mixed-spin Blume-Capel model on SC and BCC lattices with $S = 1, 2$, and 3 . The critical temperature T_C was obtained by the crossing of Binder cumulant of lattices with different sizes. This method can be used in first-order as well as continuous phase transitions [47] (see Figs. 2 and 3). Binder cumulant was calculated by two methods: Solid curves and symbols in Fig. 1 represent results from the WL and MU, respectively. They are consistent with each other within 1%. For the WL method, the lattice size is limited to $L = 4, 6$, and 10 for $S = 1$, and $L = 4$ and 6 for $S > 1$; for the MU, much larger lattices ($L = 32$ and 60) were used. We estimate that the error by the correction to scaling [3], if it exists, is small because the two results by the WL and MU methods are very close to each other.

In the phase diagram, there are a few qualitatively different regimes according to the value of Δ . For sufficiently large negative crystal field ($\Delta \rightarrow -\infty$), the system undergoes a continuous transition at a nearly constant value of T_C shown in the figures by a horizontal line. Because low-spin states ($|S_i| < S$) are suppressed in Λ_2 sites, the model is reduced into the conventional two-state Ising model with spin-1/2 and spin- S in each sublattice. We confirmed that the critical temperature converges to $T_C = (S/2)T_C^{\text{Ising}}$ in the limit $\Delta \rightarrow -\infty$ within error bars, which corresponds to the critical temperature of the conventional Ising model: $J/k_B T_C^{\text{Ising}} = 0.221654626(5)$ for the SC lattice [3] and $J/k_B T_C^{\text{Ising}} = 0.1573725(6)$ for the BCC lattice [48,49]. On the other hand, for $\Delta > \Delta_{\text{crit}}$ the vacancies ($S_j = 0$) become dominant and no long-range order occurs in the system since a spin σ_i in Λ_1 is surrounded by vacancies. In fact, the Λ_1 spins are randomly

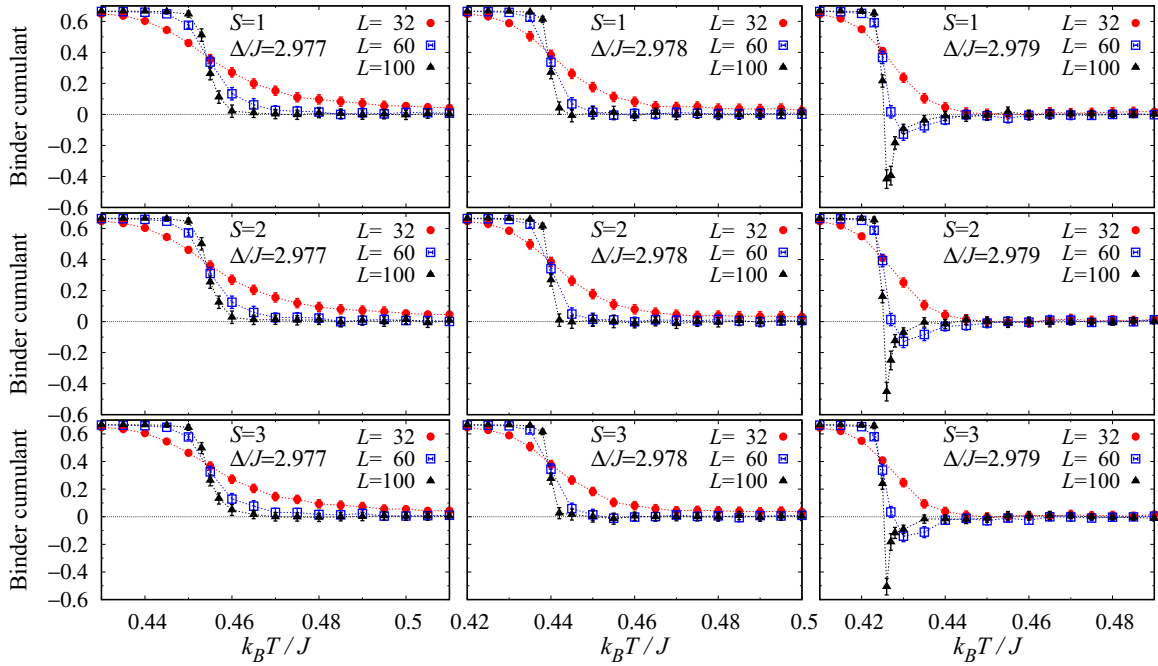


FIG. 2. Binder cumulant as a function of temperature (T) for various lattice sizes (L) in the SC lattice. Note the valley of negative value immediately above T_C for $\Delta/J = 2.979$.

oriented when the crystal field is greater than $\Delta_{\text{crit}}/J = 3$ and 4 for the SC and BCC lattices, respectively.

The most interesting part of the phase diagram is the intermediate regime, where the system changes the nature of the transition from continuous to first order, giving rise to a TCP and a line of compensation points. As Δ increases, the critical temperature decreases abruptly because nonzero spin

states in Λ_2 are reduced by the positive crystal field. As shown in Fig. 4, the reduction of $\langle M_S \rangle$ is strong near T_C and there appears the compensation point T_{comp} , where $\langle M_\sigma \rangle = \langle M_S \rangle$, below T_C . In the ferrimagnetic case ($J < 0$), the total magnetization becomes zero at T_{comp} . As usual, for vanishing T , the sublattice magnetizations $\langle M_\sigma \rangle$ and $\langle M_S \rangle$ start from their saturation values. However, one should note that in Fig. 4, M_S

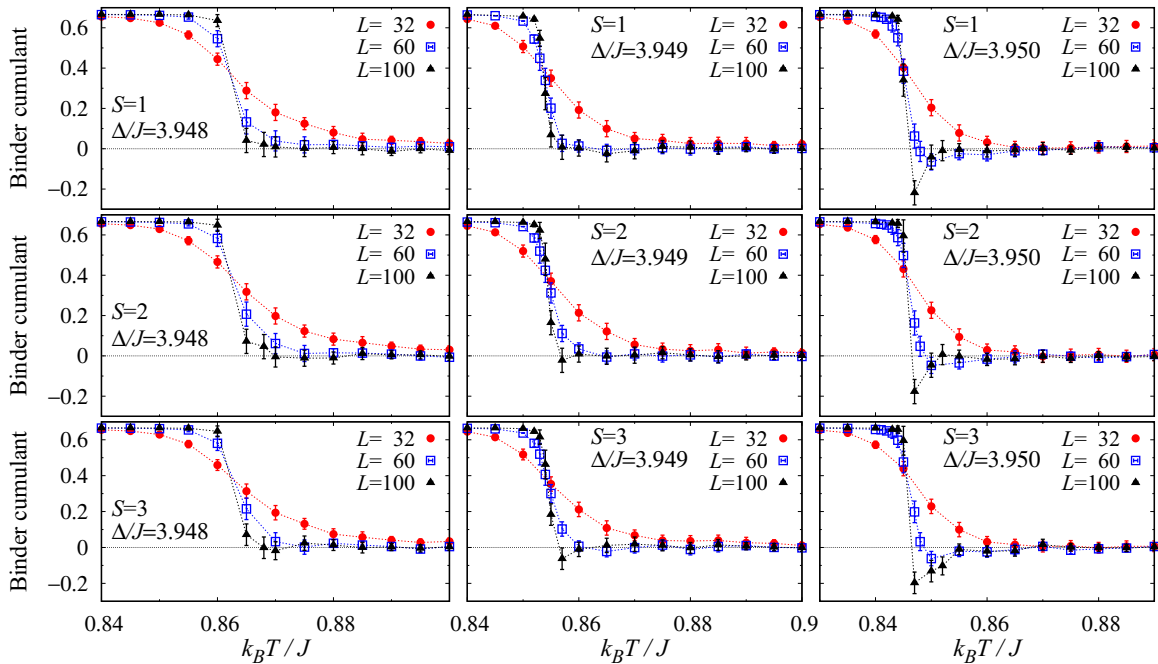


FIG. 3. Binder cumulant as a function of temperature (T) for various lattice sizes (L) in the BCC lattice. Note the valley of negative value immediately above T_C for $\Delta/J = 3.950$.

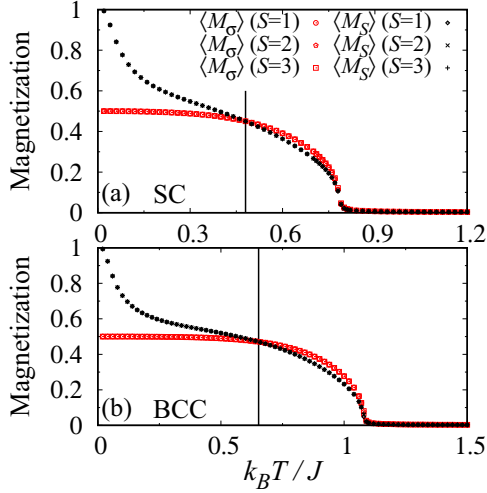


FIG. 4. Sublattice magnetizations $\langle M_\sigma \rangle$ and $\langle M_S \rangle$ as a function of temperature for the SC lattice with $\Delta/J = 2.9$ and for the BCC lattice with $\Delta/J = 3.9$. The linear size of lattices is $L = 60$. The vertical straight lines indicate the compensation point T_{comp} below the critical temperature T_C . The statistical error is smaller than the symbol size.

curves start from 1 at $T = 0$. This indicates that the states of $S_j = 1$ dominate states of $S_j = 2$ and 3 very close to the TCP. We show that the compensation appears in the BCC lattice as well as in the SC lattice [see Figs. 1(c) and 1(d)]. We found that the compensation point does not depend on the magnitude of spin S . The critical temperature and compensation lines decrease with Δ and vanish at $\Delta > \Delta_{\text{crit}}$.

To find the evidence of the discontinuous nature of the transition and to differentiate the first-order from continuous transitions, we used two methods. First, for the first-order transition, the Binder cumulant has a valley of negative values immediately above T_C , while in the case of the continuous transition, it monotonically decreases to zero as the temperature increases [47,50]. Note that the valley of the Binder cumulant can be missing in small-sized lattices even if larger lattices show it. Therefore, the existence of the valley indicates that the transition is first order, but its absence does not guarantee that the transition is continuous. Figures 2 and 3 show that $\Delta_t/J < 2.979$ and $\Delta_t/J < 3.950$ for the TCP in the SC and BCC lattices, respectively. Interestingly, Binder cumulant does not depend on the spin magnitude S around the TCP. The second method is based on the histogram of the order parameter close to T_C ; the order parameter refers to the total magnetization M in this case. For the first-order transition, the histogram of the order parameter has three peaks at $M = 0$ and $M = \pm M_0$ with $M_0 > 0$ close to T_C ; the central peak increases as temperature increases. On the other hand, in the continuous transition, there are only two peaks at $M = \pm M_0$ below T_C , and M_0 decreases as temperature increases to make only one peak at $M = 0$ above T_C . Therefore, the existence of the three-peak structure near T_C is the evidence for the discontinuity of the transition. This method was used by Selke and Oitmaa to estimate the TCP for the SC lattice with $S = 1$ [32]. However, as shown in Figs. 5 and 6, there exists a large finite-size effect in this method, too. Even when a three-peak structure is observed in small-sized lattices, it could disappear in larger lattices. For example, for $\Delta/J = 2.977$ in the SC lattice in the left column of Fig. 5, a three-peak structure is clear in $L = 10$ but it disappears for $L = 32$. Therefore, the three-peak structure does not ensure the first-order nature of

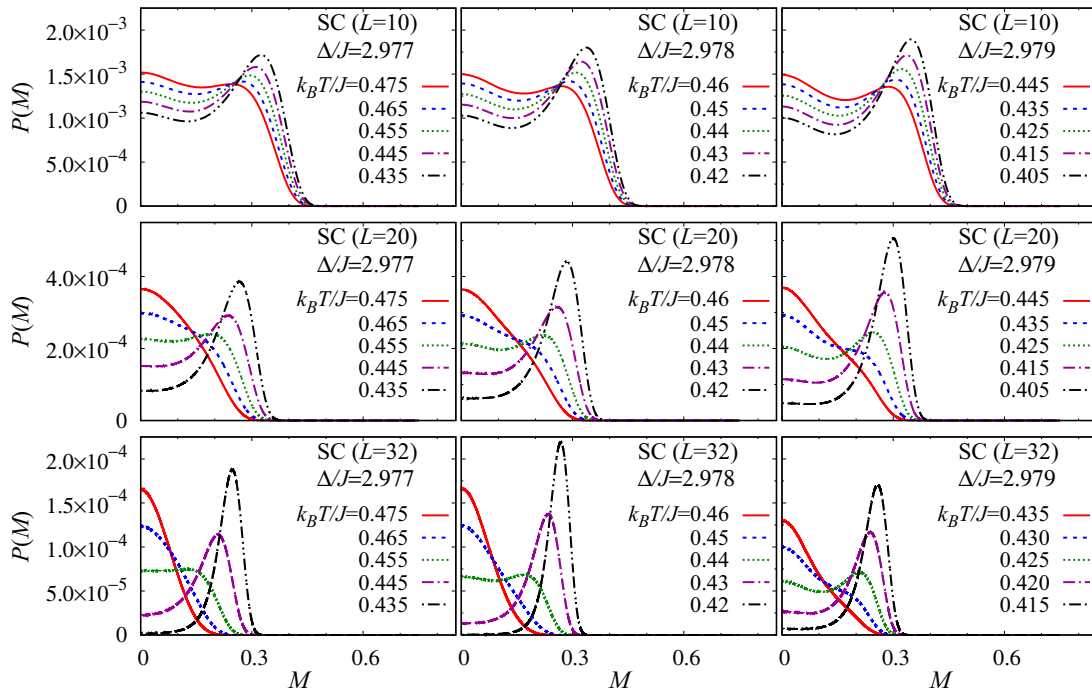


FIG. 5. Histogram of the total magnetization $P(M)$ for various values of linear size (L) at temperatures crossing the transition in the SC lattice for $S = 1$. $P(M)$ is symmetric about $M = 0$ and only results of positive M are shown.

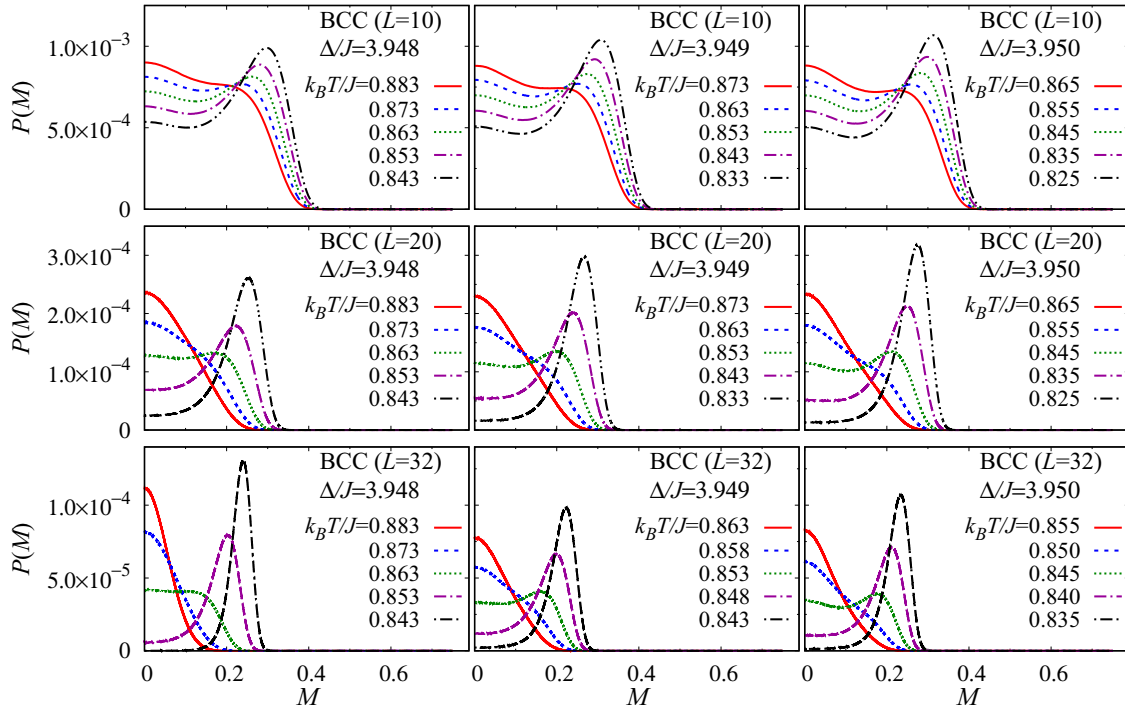


FIG. 6. Histogram of the total magnetization $P(M)$ for various values of the lattice size (L) at temperatures crossing the transition in the BCC lattice for $S = 1$. $P(M)$ is symmetric about $M = 0$ and only results of positive M are shown.

the transition, while the missing of the three-peak structure indicates that the transition is indeed continuous. As a result, we conclude that $\Delta_t/J > 2.977$ and $\Delta_t/J > 3.948$ for the SC and BCC lattices, respectively. Ignoring this effect leads to an underestimation of Δ_t/J . Previous Monte Carlo simulations are limited to small lattice sizes $L = 4$, which estimated the value of anisotropy of the TCP to be $\Delta_t/J = 2.955(15)$ [32]. Though not shown here, we obtained the same results for the cases of $S = 2$ and $S = 3$ as the $S = 1$ case within error bars. Combining the two results of the Binder cumulant and order parameter histogram, our final conclusion is that $2.977 < \Delta_t/J < 2.979$ and $3.948 < \Delta_t/J < 3.950$ for the SC and BCC lattices, respectively. Therefore, we estimate the tricritical point as $[\Delta_t/J = 2.978(1); k_B T_t/J = 0.439(1)]$ and $[\Delta_t/J = 3.949(1); k_B T_t/J = 0.854(1)]$ for the SC and BCC lattices, respectively. Note that the position of the TCP is independent of the spin magnitude S .

To understand the independence of the TCP on S , we examined $\langle n_S \rangle$, which is the portion of spin state $S_j = \pm S$ in sublattice Λ_2 , as a function of temperature. We concentrate on the case $S = 3$. Figure 7 shows $\langle n_S \rangle$ as a function of temperature for $\Delta = \Delta_t$ in the SC lattice with $S = 3$. The size dependence is very small except around T_C . At very high temperature above T_C , $\langle n_0 \rangle$ approaches $1/7$ and $\langle n_1 \rangle$, $\langle n_2 \rangle$, and $\langle n_3 \rangle$ approach $2/7$, as expected. As the temperature decreases, high-spin states ($|S_j| > 1$) are fully suppressed well above T_C and so they have no role in the transition at the tricritical point. Therefore, it is natural that the cases of $S = 2$ and $S = 3$ have the same tricritical point as the case of $S = 1$. Below T_C , $\langle n_1 \rangle$ reaches 1 smoothly; this behavior is contrary to the Blume-Capel model, where $\langle n_1 \rangle$ jumps abruptly to 1 immediately below T_C [15]. We confirmed the same behavior also around first-order transitions with larger Δ . The discrepancy may be

explained by the existence of two interpenetrating sublattices in our model coupled to each other via the interaction J . One of these sublattices is occupied by $\sigma_i = \pm 1/2$, which tries to force the spin of the last sublattice to be aligned (ferromagnetic) or antialigned (ferrimagnetic).

Finally, as the value of Δ increases passing through the TCP, continuous phase transition changes into first-order transition. At first-order transitions, canonical simulations such as MU may be trapped in a metastable phase, giving rise to the supercritical slowing down and hysteresis phenomena. It becomes more serious as Δ approaches Δ_{crit} , for larger S , and in larger lattices. The hysteresis also depends on the number of MC steps and the speed of temperature change. We observed no hysteresis in continuous transitions and close to the tricritical point. In Fig. 8, we present the thermal dependence of the

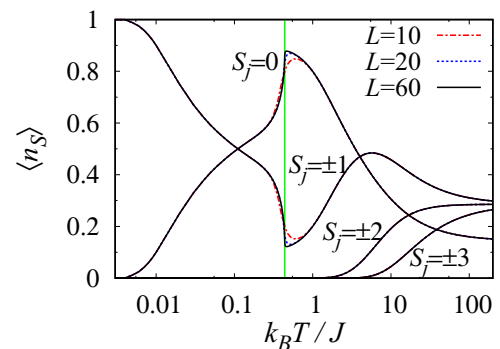


FIG. 7. Density of each spin state $\langle n_S \rangle$ as a function of temperature for $\Delta/J = 2.978$ and $S = 3$ in the SC lattice. The vertical straight line represents the transition temperature.

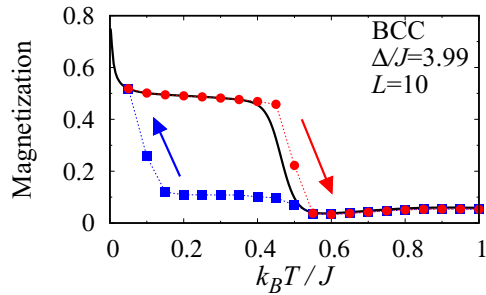


FIG. 8. Total magnetization as a function of temperature in the BCC lattice for $S = 1$, $\Delta/J = 3.99$, and $L = 10$ calculated by the MU (symbols). Squares and circles were obtained during cooling-down and warming-up processes, respectively. At each temperature, 2×10^5 MC steps were performed; the former 10^5 steps were discarded and only the later 10^5 steps were used to calculate total magnetization. Results of independent 100 runs were averaged for each process. The results by the WL sampling are plotted by the solid line for comparison. The statistical error is smaller than the symbol size.

total magnetization while increasing and lowering temperature obtained by the MU in the BCC lattice for $\Delta/J = 3.99$ and $L = 10$, which shows a very strong hysteresis effect even in a relatively small lattice. More MC steps may reduce the hysteresis effect, but we verified the existence of hysteresis at least up to 2×10^7 MC steps per each temperature value in this case. The hysteresis behavior is also observed in the SC lattice, but it is more pronounced in the BCC lattice: In the SC lattice, a clear hysteresis behavior begins to appear at $\Delta/J = 2.999$ for $L = 20$ and $S = 1$. We think that the serious hysteresis in the BCC lattice appears preferably due to the larger coordination number, which makes the metastable states deeper. Therefore, the MU should be used with special care for $\Delta > \Delta_t$. The WL method overcomes the supercritical slowing down and hence no hysteresis is observed, demon-

strating the effectiveness of the extended ensemble method in the mixed-spin systems.

IV. CONCLUSIONS

We studied the mixed spin-1/2 and spin- S Blume-Capel model with $S = 1, 2$, and 3 on three-dimensional lattices (SC and BCC) using the MU and the WL sampling to construct phase diagrams. Although the WL sampling is restricted to small-sized lattices, the results by the two algorithms coincide and the error by the correction to scaling is estimated to be small (a relative error of at most 1%). In the WL method, thermodynamic quantities at arbitrary temperature and single-site anisotropy Δ can be obtained by just one calculation and there is no supercritical slowing down. Therefore, it is now clear that the WL scheme is very efficient to study mixed-spin systems. At low values of the anisotropy Δ , the mixed-spin system shows critical lines for each integer S , which end in first-order transition lines, and they meet at the TCP (Δ_t/J ; $k_B T_t/J$). From the Binder cumulant and the histogram of magnetization as a function of temperature, we determined the TCP with very high precision as [$\Delta_t/J = 2.978(1)$; $k_B T_t/J = 0.439(1)$] and [$\Delta_t/J = 3.949(1)$; $k_B T_t/J = 0.854(1)$] for the SC and BCC lattices, respectively. The location of the TCP was determined by the MU, since large-sized lattices need to be examined due to finite-size effects. We found that the location of the TCP is independent of S because higher spin states of $|S_j| > 1$ are suppressed close to the TCP, which is confirmed by the density of each spin state $\langle n_S \rangle$ as a function of temperature. In addition, we demonstrated the existence of the line of compensation points in both lattices, which is also S independent.

ACKNOWLEDGMENTS

This work was supported by GIST Research Institute (GRI) grant funded by the GIST in 2020. A.M. would like to express his sincere thanks to Professor Walter Selke for the valuable discussions and advice.

-
- [1] E. Ising, *Z. Phys.* **31**, 253 (1925).
 - [2] L. Onsager, *Phys. Rev.* **65**, 117 (1944).
 - [3] A. M. Ferrenberg, J. Xu, and D. P. Landau, *Phys. Rev. E* **97**, 043301 (2018).
 - [4] M. Blume, *Phys. Rev.* **141**, 517 (1966).
 - [5] H. W. Capel, *Phys. (Amsterdam, Neth.)* **32**, 966 (1966).
 - [6] W. Selke and J. Yeomans, *J. Phys. A: Math. Gen.* **16**, 2789 (1983).
 - [7] W. Selke, D. A. Huse, and D. M. Kroll, *J. Phys. A: Math. Gen.* **17**, 3019 (1984).
 - [8] N. G. Fytas and W. Selke, *Eur. Phys. J. B* **86**, 365 (2013).
 - [9] N. G. Fytas, A. Mainou, P. E. Theodorakis, and A. Malakis, *Phys. Rev. E* **99**, 012111 (2019).
 - [10] P. D. Beale, *Phys. Rev. B* **33**, 1717 (1986).
 - [11] M. Deserno, *Phys. Rev. E* **56**, 5204 (1997).
 - [12] C. J. Silva, A. A. Caparica, and J. A. Plascak, *Phys. Rev. E* **73**, 036702 (2006).
 - [13] N. G. Fytas, *Eur. Phys. J. B* **79**, 21 (2011).
 - [14] J. Zierenberg, N. G. Fytas, and W. Janke, *Phys. Rev. E* **91**, 032126 (2015).
 - [15] W. Kwak, J. Jeong, J. Lee, and D.-H. Kim, *Phys. Rev. E* **92**, 022134 (2015).
 - [16] M. Jung and D.-H. Kim, *Eur. Phys. J. B* **90**, 245 (2017).
 - [17] P. Butera and M. Pernici, *Phys. A (Amsterdam, Neth.)* **507**, 22 (2018).
 - [18] D. P. Landau and R. H. Swendsen, *Phys. Rev. Lett.* **46**, 1437 (1981).
 - [19] B. A. Berg and T. Neuhaus, *Phys. Lett. B* **267**, 249 (1991).
 - [20] B. A. Berg and T. Neuhaus, *Phys. Rev. Lett.* **68**, 9 (1992).
 - [21] L. Néel, *Ann. Phys.* **12**, 137 (1948).
 - [22] M. Drillon, E. Coronado, D. Beltran, and R. Georges, *Chem. Phys.* **79**, 449 (1983).
 - [23] C. Mathonière, C. J. Nuttall, S. G. Carling, and P. Day, *Inorg. Chem.* **35**, 1201 (1996).

- [24] T. Kaneyoshi, *J. Phys. Soc. Jpn.* **56**, 2675 (1987).
- [25] N. Benayad, A. Klümper, J. Zittartz, and A. Benyoussef, *Z. Phys. B* **77**, 339 (1989).
- [26] N. Benayad, *Z. Phys. B* **81**, 99 (1990).
- [27] T. Kaneyoshi and J. Chen, *J. Magn. Magn. Mater.* **98**, 201 (1991).
- [28] G.-M. Zhang and C.-Z. Yang, *Phys. Rev. B* **48**, 9452 (1993).
- [29] A. Bobák and M. Jurčičin, *Phys. A (Amsterdam, Neth.)* **240**, 647 (1997).
- [30] G. M. Buendía and M. A. Novotny, *J. Phys.: Condens. Matter* **9**, 5951 (1997).
- [31] J. Oitmaa and I. G. Enting, *J. Phys.: Condens. Matter* **18**, 10931 (2006).
- [32] W. Selke and J. Oitmaa, *J. Phys. Condens. Matter* **22**, 076004 (2010).
- [33] A. Dakhama, M. Azhari, and N. Benayad, *J. Phys. Commun.* **2**, 065011 (2018).
- [34] L. L. Gonçalves, *Phys. Scr.* **32**, 248 (1985).
- [35] A. Dakhama, *Phys. A (Amsterdam, Neth.)* **252**, 225 (1998).
- [36] G. M. Buendía and R. Cardona, *Phys. Rev. B* **59**, 6784 (1999).
- [37] N. Metropolis, A. W. Rosenbluth, M. N. Rosenbluth, A. H. Teller, and E. Teller, *J. Chem. Phys.* **21**, 1087 (1953).
- [38] S. G. A. Quadros and S. R. Salinas, *Phys. A (Amsterdam, Neth.)* **206**, 479 (1994).
- [39] F. Wang and D. P. Landau, *Phys. Rev. Lett.* **86**, 2050 (2001).
- [40] A. Kumar and S. Yusuf, *Phys. Rep.* **556**, 1 (2015).
- [41] W. Janke, in *Computer Simulation Studies in Condensed-Matter Physics VII*, edited by D. P. Landau, K. K. Mon, and H.-B. Schüttler (Springer, Berlin, 1994), p. 29.
- [42] M. Azhari, N. Benayad, and M. Mouhib, *Superlattices Microstruct.* **79**, 96 (2015).
- [43] S.-H. Tsai, F. Wang, and D. P. Landau, *Phys. Rev. E* **75**, 061108 (2007).
- [44] C. Zhou, T. C. Schulthess, S. Torbrügge, and D. P. Landau, *Phys. Rev. Lett.* **96**, 120201 (2006).
- [45] U. Yu, *Phys. Rev. E* **91**, 062121 (2015).
- [46] K. Binder, *Z. Phys. B* **43**, 119 (1981).
- [47] M. S. S. Challa, D. P. Landau, and K. Binder, *Phys. Rev. B* **34**, 1841 (1986).
- [48] P. Butera and M. Comi, *Phys. Rev. B* **62**, 14837 (2000).
- [49] P. H. Lundow, K. Markström, and A. Rosengren, *Phil. Mag.* **89**, 2009 (2009).
- [50] K. Vollmayr, J. D. Reger, M. Scheucher, and K. Binder, *Z. Phys. B* **91**, 113 (1993).